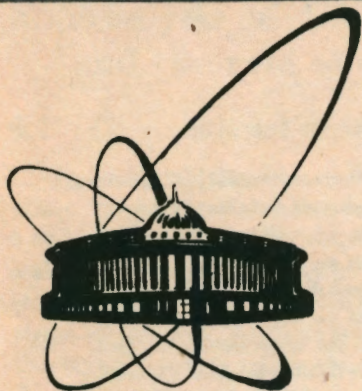


92-138



ОБЪЕДИНЕННЫЙ
ИНСТИТУТ
ЯДЕРНЫХ
ИССЛЕДОВАНИЙ
ДУБНА

E4-92-138

A.S.Dem'yanova¹, E.F.Svinareva, S.A.Goncharov²,
S.N.Ershov, F.A.Gareev, G.S.Kazacha, A.A.Ogloblin¹,
J.S.Vaagen³

SCATTERING OF ^3He ON ^{12}C
AND INELASTIC FORM FACTOR

Submitted to "Nuclear Physics"

¹The Kurchatov Institute of Atomic Energy, Moscow, Russia

²Nuclear Research Institute of Moscow State University, Russia

³Institute of Physics, University of Bergen, Norway

1992

1 Introduction

The discovery of nuclear rainbow effects in direct nuclear reactions [1]-[4] opened new possibilities to investigate internuclear interactions at shorter distances. Contrary to the elastic scattering, a reaction cross section depends not only on the nucleus-nucleus potential, but also on the reaction form factor. This gives a chance to test the wave functions of the nuclei participating in a reaction at small distances corresponding to the rainbow trajectories. The form factors themselves on the other hand, also influence the contribution of the various partial waves to the cross section, so that the reaction becomes a supplementary tool for exploring the nucleus-nucleus potential. Both aspects were documented in our studies of the reactions ($^3\text{He}, t$) and ($^6\text{Li}, ^6\text{He}$) on carbon isotopes [2, 3, 5, 6].

One of the simplest processes in which rainbow effects could be expected is inelastic scattering. Rainbow-like behaviour of the differential cross sections both of elastic and inelastic scattering, beyond the oscillations of the Fraunhofer forward-angle diffraction has been observed in some studies, such as [7]-[11], although there was no special analysis of rainbow phenomena in these works.

Results have however been reported [4] where the nuclear rainbow was observed in the elastic and single-nucleon transfer angular distributions of $^{12,13}\text{C}$ on ^{12}C at $E=20$ MeV/A; but not seen in the inelastic scattering of these nuclei for the 2^+ (4.44 MeV) state. For some reason the inelastic excitation was reduced in the interior. As an explanation the authors [4] suggested that inelastic form factors for $^{12,13}\text{C}+^{12}\text{C}$ are more narrowly surface localized than form factors taken proportional to the first derivative of the optical potential.

In previous publications [3, 5, 6] we have analyzed the character of rainbow effects in the interaction of ^3He with carbon nuclei. A strong dependence of the measured angular distributions on the radial behaviour of the form factors in charge-exchange reactions ($^3\text{He}, t$) was established. This leads us to expect that for inelastic scattering the cross section should be sensitive to the radial dependence of the form factor too.

In spite of the presence of a nuclear rainbow, potential ambiguities remained in our previous analysis of elastic data, but appeared partly solved when a fit to both elastic and charge-exchange data was required. With the aim of exploring these questions further special experiments were carried out to measure the inelastic scattering cross sections of $^3\text{He}+^{12}\text{C}$ at 72 MeV.

2 Measurements

The measurements with a beam of 72 MeV (lab) helions were carried out at the isochronous cyclotron of the Kurchatov Institute of Atomic Energy. The inelastically scattered particles were detected with a (ΔE -E) telescope. Self-supporting targets of carbon were used. The conditions of the experiment were similar to those of the previous study of elastic scattering of ^3He on carbon isotopes [3, 6]. A brief report on the experimental data was given in [12].

3 Analysis of $^3\text{He}+^{12}\text{C}$ inelastic scattering data and the role of a nuclear rainbow

3.1 Conventional analysis with the A2 potential

Figure 1 gives the measured differential cross sections of elastic and inelastic scattering $^3\text{He}+^{12}\text{C}$ with excitation of the low lying 4.44 MeV (2^+), 7.65 MeV (0^+), 9.64 MeV (3^-) states of the target. The angular distributions of the elastic and inelastic scattering have similar features: a diffraction structure at small angles, followed by an almost exponential fall-off with approximately equal slopes in all cases and finally the region at very large angles in which rather strong oscillations reappear. In the diffraction region the data satisfy the well known Blair phase rule. In our recent analysis of the elastic scattering [6] we showed that the behaviour of the cross section at angles beyond the diffractive oscillations, corresponds to rainbow scattering. Fig. 1 shows the elastic scattering calculation with the potential A2 from [6]. Thus the very shape of the angular distributions for the 4.44 MeV 2^+ -state indicates qualitatively that inelastic scattering of ^3He on ^{12}C at $E/A \sim 25$ MeV/A contains distinct features of the nuclear rainbow.

To substantiate this inference we have carried out quantitative analyses of inelastic scattering $^3\text{He}+^{12}\text{C}$ with excitation of 2^+ and 3^- states, both within the DWBA and coupled channels approximation (CC).

The relative motions were described with standard form Wood-Saxon and derivative optical potentials. The best one-channel fit parameters (A2) to the elastic scattering are given in table 1. For the imaginary part a combination of volume and surface absorption was adopted as the most adequate form [2, 6].

Table 1. Parameters for Woods-Saxon type optical potentials used for describing the elastic scattering data $^3\text{He}+^{12}\text{C}$ at $E_{^3\text{He}} = 72 \text{ MeV}$.

N	-V	r_V^*	a_V	-W	r_W	a_W	W_D	r_D	a_D
A2	112.5	0.860	0.830	3.50	2.69	0.452	5.65	1.16	0.411
A4	112.8	1.103	0.831	4.58	2.17	0.98	9.90	1.268	0.550

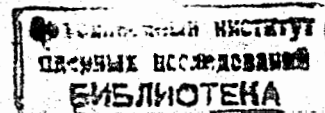
N	V_{SO}	r_{SO}	a_{SO}	$\frac{J_V}{3A_T}$	$\frac{J_W}{3A_T}$	$\langle r_V^2 \rangle^{1/2}$	$\langle r_W^2 \rangle^{1/2}$	$\frac{\chi^2}{N}$	σ_R
A2	0.31	1.40	0.191	275	125	3.44	5.05	3.8	962
A4	0.39	1.264	0.107	437	161	3.65	4.64	6.4	1065

*) $R_i = r_i A_T^{1/3}$, $r_C = 1.4$ fm; $r_C = 1.25$ fm for A4

As a starting point we choose inelastic form factors (for the 2^+ and 3^- states) proportion to derivatives of the optical potential

$$F_L^d(U; R) = \beta_L f_L^d(U; R) = (\beta_L R_V) \frac{dU(R)}{dR} \quad (1)$$

This is, as is well known, the leading term if a collective model description were appro-



appropriate. The transition to the more complicated 0^+ state was left out of our analysis in this paper.

The deformation parameter β_L was taken as a free parameter. The values of β_2 and β_3 as well as deformation lengths $\beta_L R_V$ obtained below (see tabl.2) are in good agreement with the results of other authors, for example [9, 13]. The authors of [13] found for the scattering $\alpha + {}^{12}\text{C}$ at $E_\alpha = 104$ MeV the value $\beta_2 R_V = 1.07 \pm 0.05$ fm. In our case the corresponding values fall between 1.02 to 1.41 fm for different choices of the potential.

Table 2. Renormalization of optical model parameters for elastic and inelastic scattering ${}^3\text{He} + {}^{12}\text{C}$ from DWBA to coupled channels analysis.

	J^π	V	W	W_D	β_l	$\beta_l R_V$	$\frac{\beta_l R_V}{a_V}$	χ^2/N
	0^+	112.5	3.50	5.65	-	-	-	3.9
DWBA	2^+	-	-	-	0.56	1.10	1.33	14.8
	3^-	-	-	-	0.35	0.69	0.83	23.8
	0^+	113.1	2.72	5.58	-	-	-	10.0
CC	2^+	-	-	-	0.52	1.02	1.23	11.7
	3^-	-	-	-	0.33	0.65	0.78	20.5
	0^+	112.8	4.577	9.904	-	-	-	6.4
DWBA	2^+	-	-	-	0.56	1.41	1.70	6.3
	3^-	-	-	-	0.35	0.88	1.06	24.9

The results of DWBA calculations with optical potential A2 and form factors $F_L^d(A2; R)$, for the inelastic scattering to 2^+ and 3^- states are shown in Fig.2a by solid lines. The potential A2 proposed by us in [6] reproduces very well the elastic scattering ${}^3\text{He} + {}^{12}\text{C}$, and its analogues B2 and C2 also the $({}^3\text{He}, t)$ reactions on ${}^{13}\text{C}$ and ${}^{14}\text{C}$. The fit to the inelastic scattering data is not quite as good as for the elastic (see discussion below).

To reveal the presence of the nuclear rainbow effect in the inelastic scattering, we used the standard decomposition of the scattering amplitude into nearside and farside components and as a test we also put the imaginary part of the potential equal to zero in the farside component. As can be seen in Fig. 2a the cross sections at angles $\sim 30^\circ - 100^\circ$ are mainly connected with the farside components (long-dashed lines in Fig. 2a). If the absorption is removed, the cross sections in this region increase significantly and form broad shoulders. A remnant of this is present in the experimental data. In the near-far decomposition of the elastic scattering [6], a prominent bump in the same domain of the elastic angular distribution was identified with a rainbow Airy maximum. The Airy maximum in the farside components of inelastic cross sections as $W \rightarrow 0$ turns out to be less prominent than for the elastic scattering. This reflects the influence of the form factor on the contributions of different partial waves to the rainbow maximum.

Thus, the analysis of the experimental data on the basis of "standard" DWBA calculations substantiate our previous qualitative conclusion: The inelastic scatterings

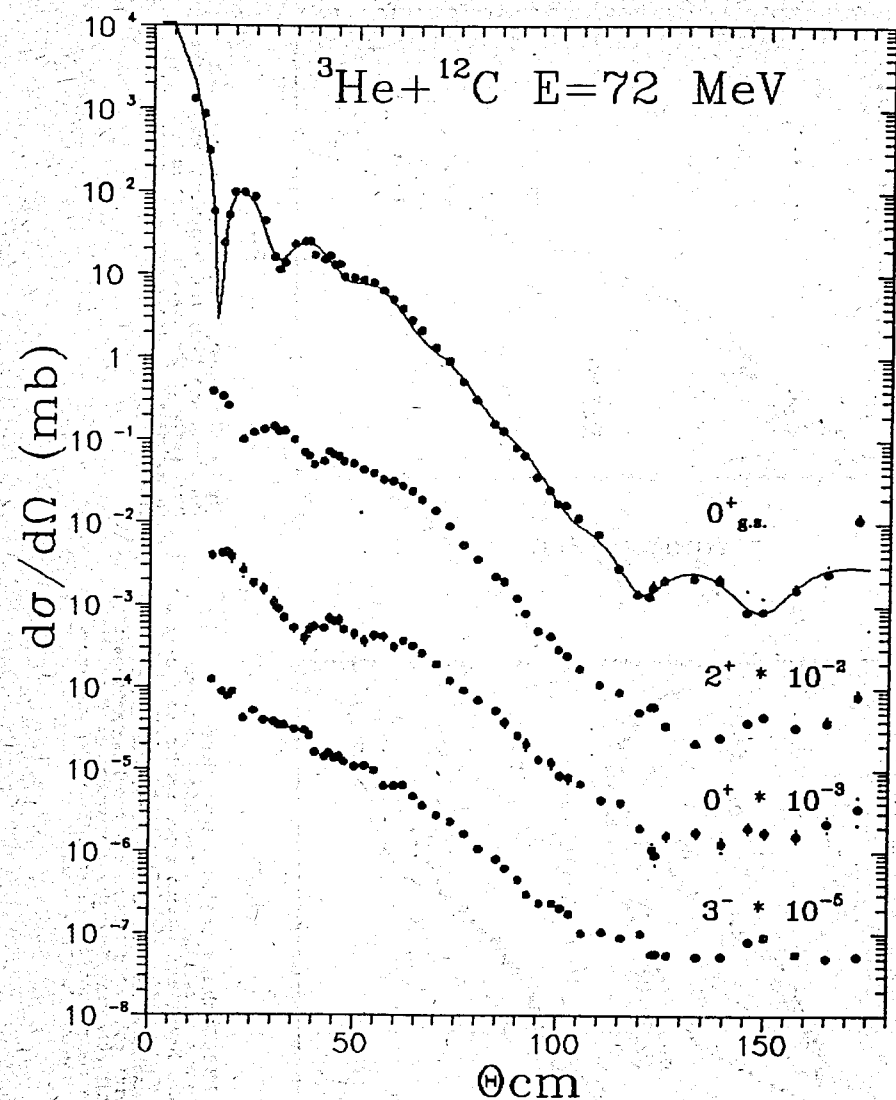


Fig 1. Experimental elastic and inelastic cross sections ${}^3\text{He} + {}^{12}\text{C}$ at $E=72$ MeV. Theoretical cross section for optical potential A2 are shown by solid line.

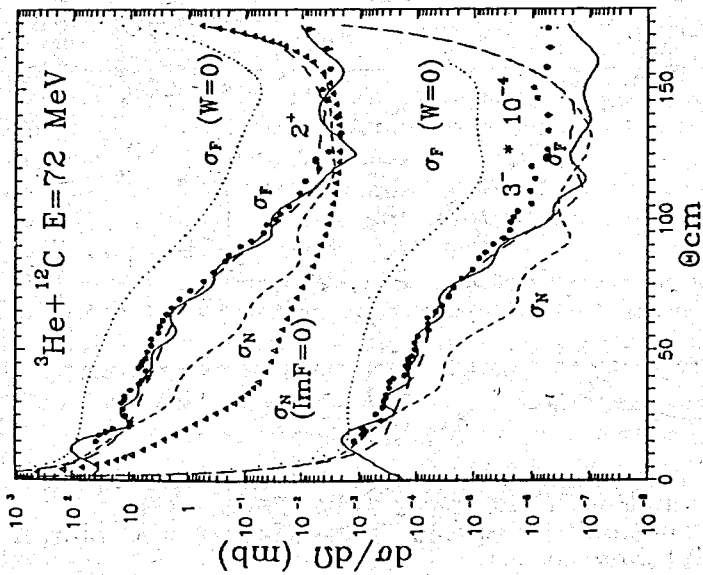


Fig 2a. DWBA inelastic angular distributions for the optical potential A2 (solid lines) compared with data. Near- and farside cross section components are shown by short- and long-dashed lines correspondingly. The dotted line shows the farside component calculated leaving out the imaginary part of optical potential. Triangles correspond to the nearside component calculated without the imaginary part of the excitation form factor.

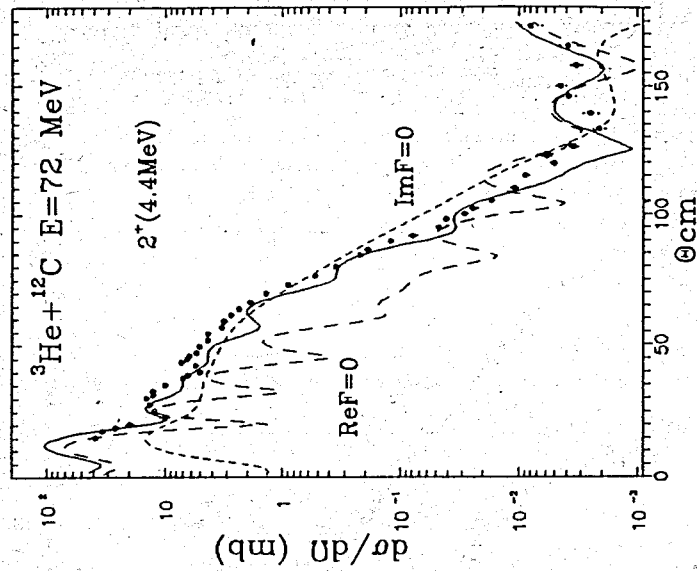


Fig 2b. The separate contributions from real (short-dashed line) and imaginary (long-dashed line) parts of the inelastic form factor (potential A2) to the inelastic 2^+ cross section.

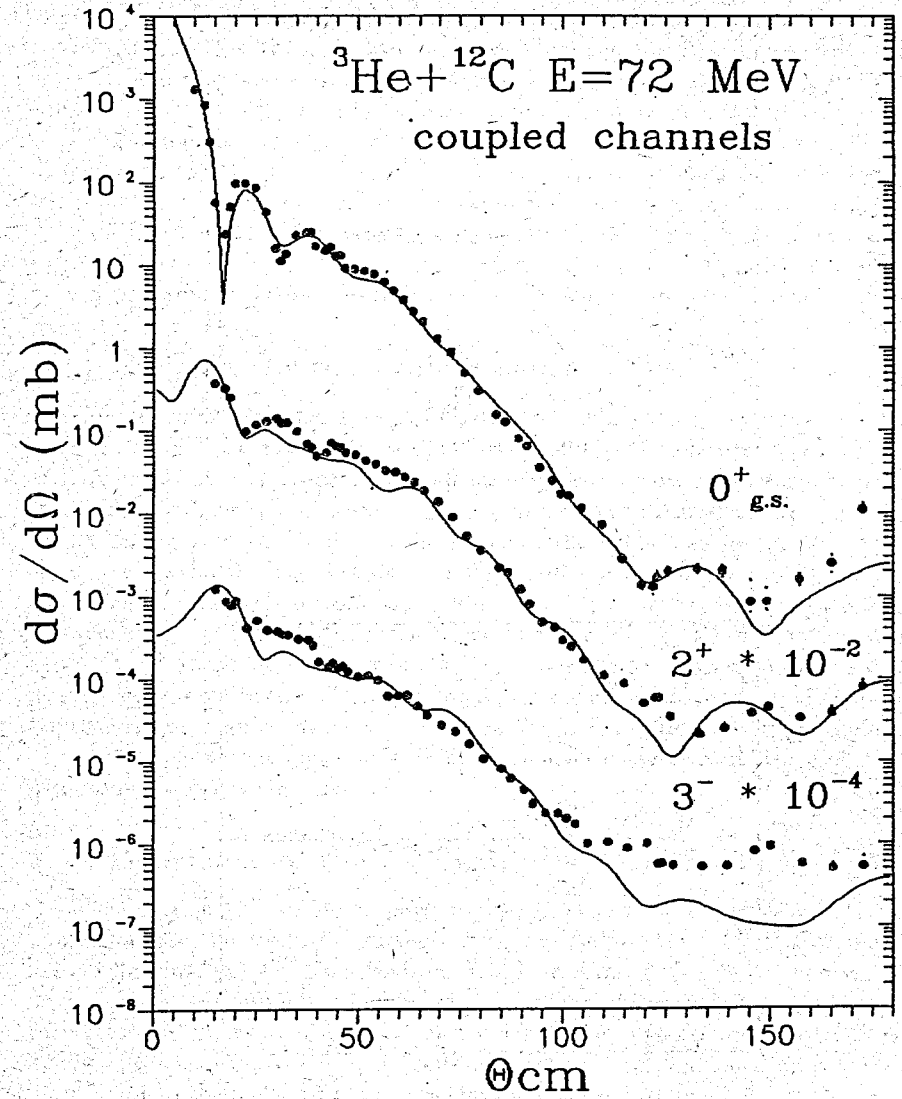


Fig 3. Coupled channel calculations of elastic and inelastic cross sections based on potential A2.

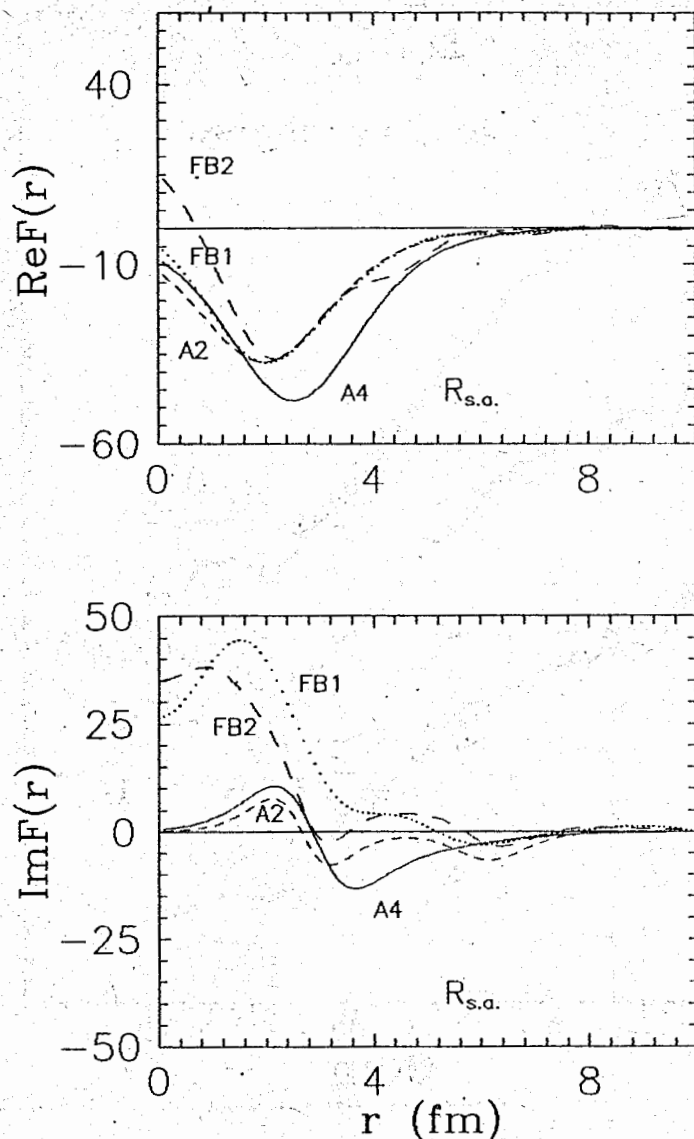


Fig. 4. Comparison of derivative inelastic form factors for potentials A2 and A4 (short-dashed and solid lines respectively) with model independent form factors based on A2 potential. Dotted and long dashed lines correspond to first FB1 and second FB2 way of including Fourier-Bessel series.

of ${}^3\text{He} + {}^{12}\text{C}$ at $E=72$ MeV with the excitation of several low lying states of the target contain the presence of a nuclear rainbow. The general description of the inelastic cross sections obtained with the A2 potential and a derivative excitation form factor is satisfactory, but looking at details there is room for improvements in particular at small angles. Compared with both the experimental data and the calculated elastic angular distribution, the diffractive oscillations of the calculated inelastic cross sections are too pronounced and rapid. Moreover, the oscillations cover the whole angular range. This disagreement may be cured by (i) replacing the DWBA by a CC treatment, (ii) modifying the recipe for the inelastic form factors, (iii) replacing A2 by another optical potential, or some combination of (i-iii). We have explored these possibilities.

3.2 Coupled channels calculations

Coupled channels calculations of elastic and inelastic cross sections were done for the $0_{g.s.}^+$, 2^+ and 3^- states. The results are shown in Fig. 3 in comparison with the experimental data. The same renormalization of optical potentials was performed in all the included channels. As a result, the real depth of the potential was almost unchanged but the imaginary part was decreased due to the explicit inclusion of two inelastic states (see table 2). This results in a slight difference between the DWBA and CC form factors, using (1). In comparison with DWBA, the coupled channels calculations dampened the oscillations somewhat, thus slightly improved the description for the 2^+ state (the χ^2 value decreased, see in table 2). For the 3^- state the agreement did not become noticeably better. Thus the coupled channels calculations practically did not improve the description of inelastic cross sections. We obtained similar results for the other elastic-equivalent potentials of [6]. The main disagreement, the high frequency oscillations, was not removed.

3.3 Deficiency of the A2 derivative form factor

The imaginary form factor part derived from the A2 potential by (1) becomes nonmonotonous in the region of the strong absorption radius ($R_{s.a.} \simeq 5.5\text{fm}$) (short dashed line in Fig. 4). This leads to a modification of the distorted waves by the form factor in the diffraction region which consequently lead to the appearance of the enhanced oscillations, absent in the elastic scattering cross section. This is illustrated in Fig. 2b where individual contributions from the real and imaginary parts of the form factor to the inelastic 2^+ cross section are shown. At small angles the imaginary part is dominant, which becomes immediately clear from direct comparison of the form factor parts in the vicinity of $R_{s.a.}$ (Fig. 4).

The enhanced oscillatory structure can be understood from the fact that the far and near components of the inelastic cross sections interfere although with varying strength, throughout the whole angular range. The crossover takes place at about $\Theta = 20^\circ$ (Fig. 2a) because the nearside component of the inelastic cross section falls down more slowly than in the elastic; usually the crossover angle for the reactions lies

near 0° if the Coulomb excitation is not included into the form factor. If we take out the imaginary part of the inelastic form factor from the calculations, the nearside component of the cross section will decrease more rapidly (triangles in Fig. 2a) and the crossover points move close to 0° .

Thus the simple recipe of the potential A2 together with the derivative form factor (1) does not quite give the correct (asymptotic) behaviour at and beyond $R_{s.a.}$ which shows up in an unsatisfactory reproduction of the inelastic scattering diffraction structure. The rainbow bump in the inelastic scattering is however well reproduced implying that at smaller distances the form factor is quite adequate.

Potentials with larger real part volume integrals than A2 were less favored in [6] because of lower quality reproduction of the ($^3\text{He}, t$) reaction data although they also gave high quality fits to the elastic scattering. We have tried to possibly trace the lack of a fully satisfactory agreement with inelastic scattering data at small angles to a deficiency of the A2 potential, i.e. we reconsidered other sets of parameters.

The existence of several potentials which, though being considerably different in the radial region relevant for "rainbow" effects, reproduce the elastic scattering data not only in the diffraction region but also in the rainbow region, has been attributed to a new kind of the optical potential ambiguity discovered by us [5, 6] and called the "V-W" ambiguity. Refractive and absorptive power can outbalance each other, so that if the ratio $V(r)/W(r)$ is nearly the same in the "rainbow" region the positions of rainbow maxima remain nearly the same for all potentials.

We have found an alternative potential A4 starting from the real part of a potential [8] which reproduces the angular distributions of elastic and inelastic scattering $^3\text{He}+^{12}\text{C}$ at $E=82$ MeV (table 1). The A4 potential gives a somewhat inferior detailed fit to the elastic scattering compared with the A2 potential, thus is not quite elastic-equivalent, but gives the same position of the rainbow bump in the far-side component without absorption as is shown in Fig. 5. To make the slope of the cross section steeper, a stronger absorption than that of the A2 potential was introduced. The insertion into Fig. 5 shows the ratio $V(r)/W(r)$ for the A2 and A4 potentials.

Fig. 6a gives the results of DWBA calculations of the inelastic cross sections using formula (1) with the potential A4, including the near-far decomposition. The A4 potential gives an improved description of the inelastic scattering with the same deformation parameters as chosen for A2. For the A4 potential the farside and nearside components are separated considerably and the crossover point has moved to very small angles. The contribution from the imaginary part of the form factor becomes both weaker and less oscillatory (see Fig. 6b). The role of the real part of the form factor becomes more significant not only in the rainbow region, but also at small angles compared with the A2 potential (Fig. 2b).

It is useful to compare form factors derived from the A2 and A4 potentials in order to understand better the origin of the improvement of the theoretical inelastic cross sections in the latter case. Fig. 4 shows that the imaginary part of the form factor derived from A4 is monotonous and less significant than the real one in the region near $R_{s.a.}$ compared with the case of the A2 potential. As a result, the modification of

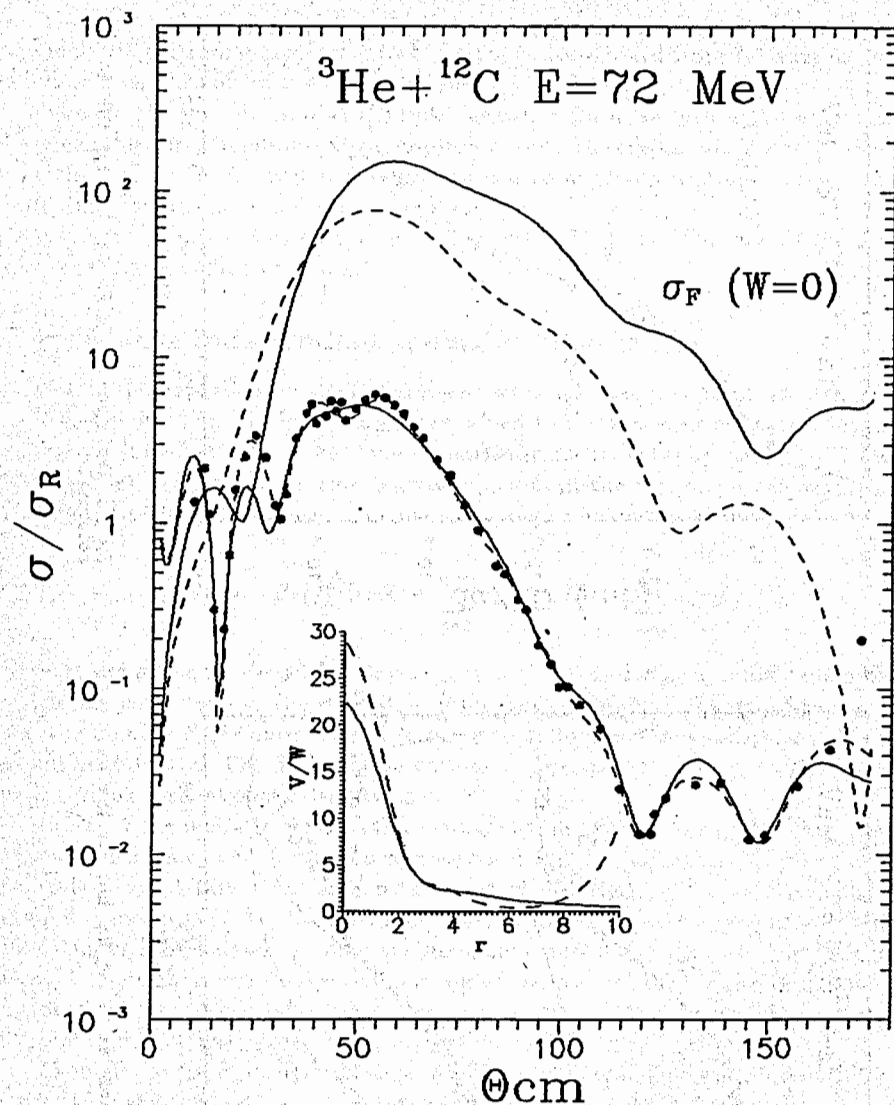


Fig 5. Theoretical elastic cross sections for the optical potential A2 (dashed line) and A4 (solid line) compared with data. The farside components of the cross section calculated without the imaginary part of potentials are also shown. The ratio of real and imaginary parts of the optical potentials A2 and A4 are inserted.

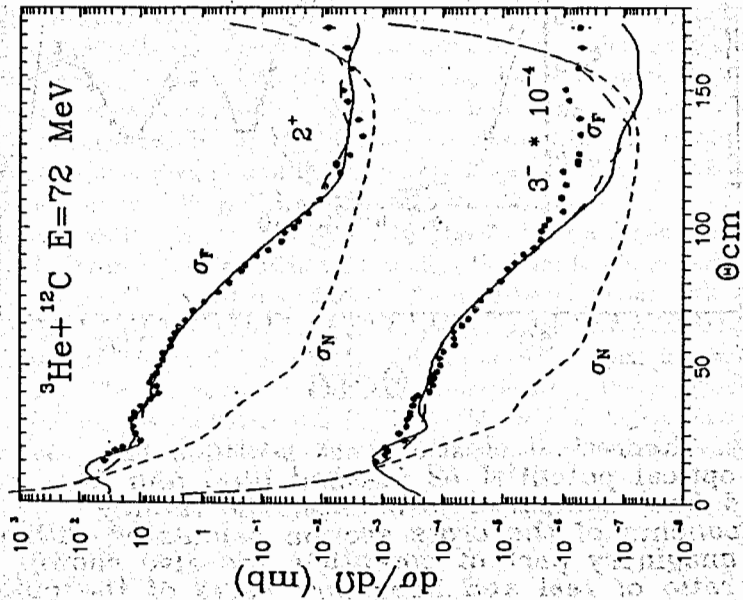


Fig 6a. The same as in Fig 2a, but for the A4 potential.

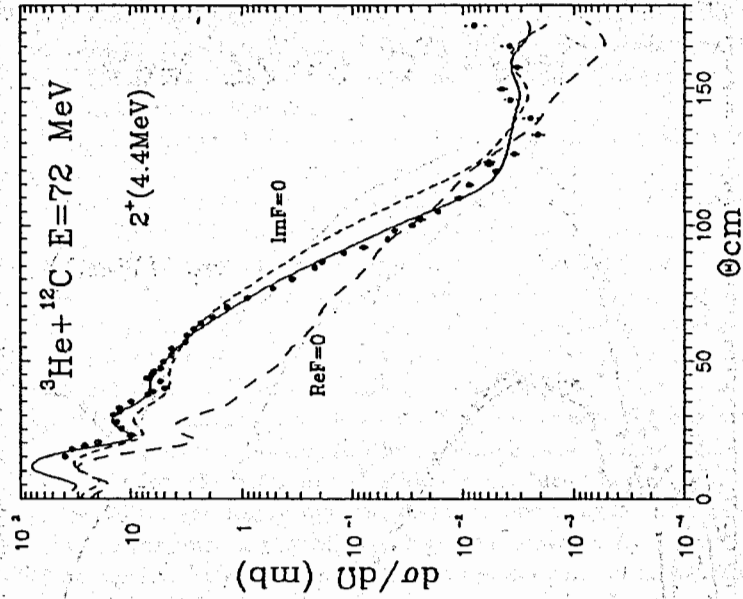


Fig 6b. The same as in Fig 2b, but for the A4 potential.

the inelastic scattering amplitude by the form factor derived from A4 does not lead to additional oscillations in the cross sections.

Thus in the framework of the simple derivative form factor, the A4 potential may be preferable for a simultaneous description of both the elastic and inelastic scattering as compared to the A2 potential, although it is somewhat a matter of taste. The two potentials are definitely not elastic-equivalent.

We have mostly discussed the excitation of the 2^+ state. The case of the 3^- state gave the same qualitative results.

3.4 Model independent inelastic form factor

A model independent analysis of inelastic scattering has been discussed, for example in [10], where a Fourier-Bessel series was added to the real collective form factor. An analogous investigation of the complex inelastic form factor is carried out here by adding Fourier-Bessel series (for generality) to both the real and imaginary parts of the derivative form factor,

$$F_L(R) = \beta_L(f_L^d(U; R) + \sum_{n=1}^N a_n j_L(q_n R) + i \sum_{n=1}^N b_n j_L(q_n R)). \quad (2)$$

Here j_L are spherical Bessel functions, $q_n = n\pi/R_{cut}$ and R_{cut} a cutoff radius beyond which the correction to the derivative form factor vanishes. The coefficients a_n , b_n and the number N of Fourier-Bessel terms were determined by least-squares fits to the experimental data. The deformation parameters β_L were kept at the values found in the previous conventional calculations.

In Fig. 7 the inelastic cross sections calculated in DWBA using both the derivative and model independent form factors are shown for the A2 potential. The model independent calculations were done with two ways of including Fourier-Bessel series. In the first procedure (FB1) the imaginary part of the form factor was fully constructed as a Fourier-Bessel series (putting the imaginary part of the derivative form factor to zero), while a Fourier-Bessel series was added to the real part of the derivative form factor. The second procedure (FB2) consists of adding Fourier-Bessel series to both the real and imaginary parts of the derivative form factor.

As might have been expected the use of model independent form factors very well reproduces the inelastic cross section (see dotted and dashed lines in Fig. 7 for the first and second way of including the Fourier-Bessel series, respectively). The real and imaginary parts of the model independent form factors are shown in Fig. 4. Using different ways to include the Fourier-Bessel series, we have also observed that the radial shape of the model independent form factor depends on the calculating procedure but that the cross sections obtained are essentially the same. Next we investigate which aspects of the form factor are responsible for the agreement with experiment.

The first type of form factor modification nearly kept the derivative real form factor unchanged, but gave a very different imaginary one giving an increased imaginary form

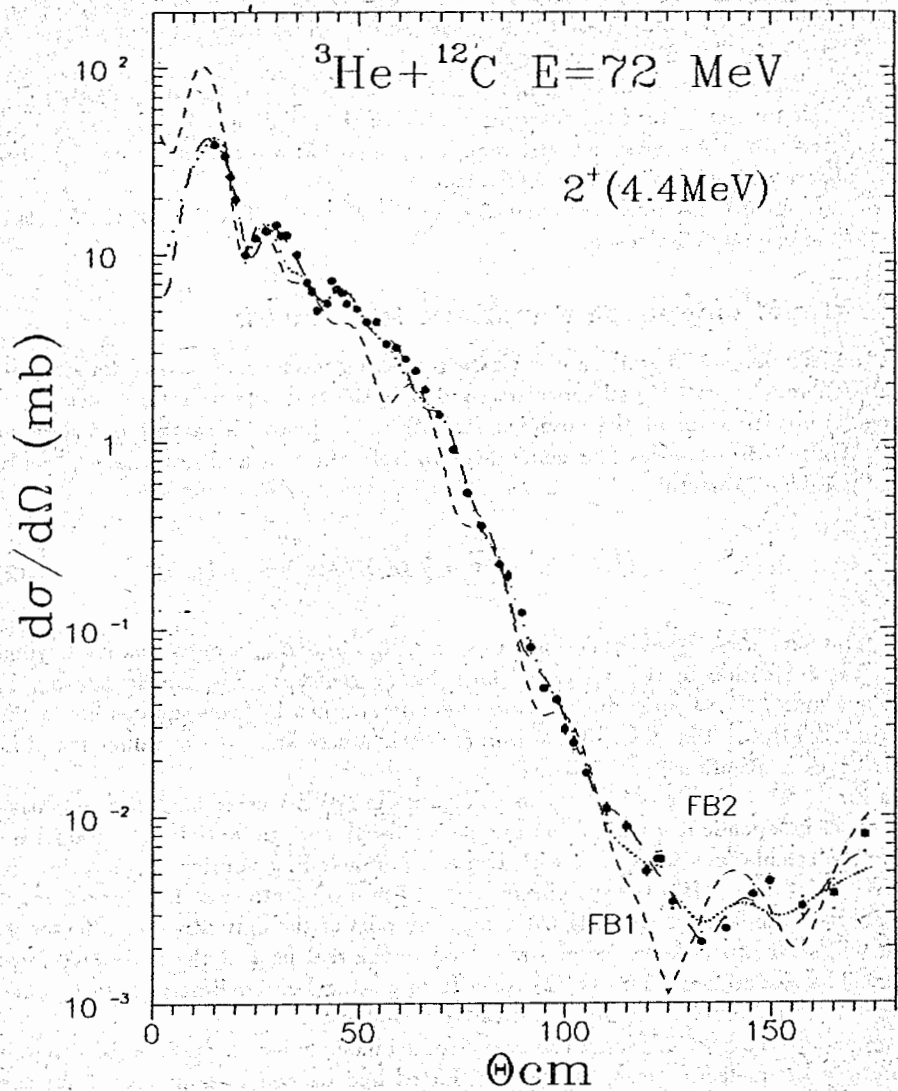


Fig 7. DWBA 2^+ cross section calculations for optical potential A2 with derivative form factor (short dashed line) and model independent form factors with first and second way of including Fourier-Bessel series (dotted and long dashed lines correspondently).

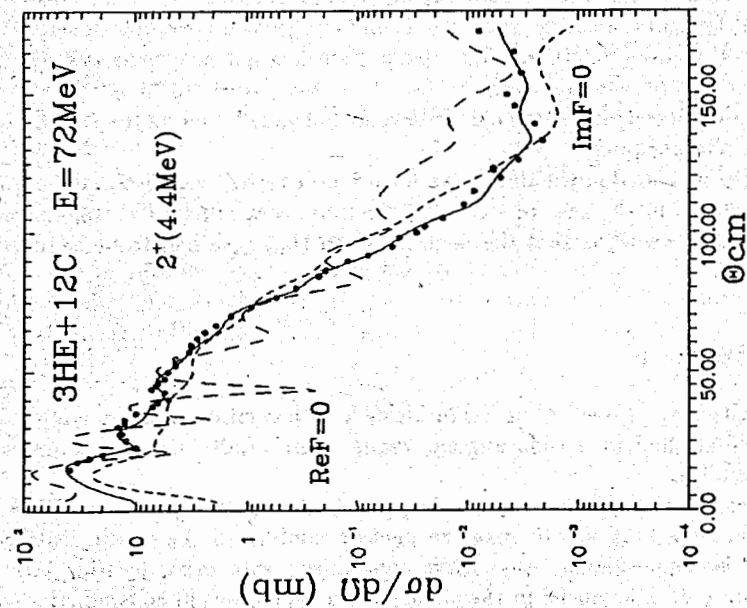


Fig 8a. The same as in Fig. 2b for the model independent form factor FB1.

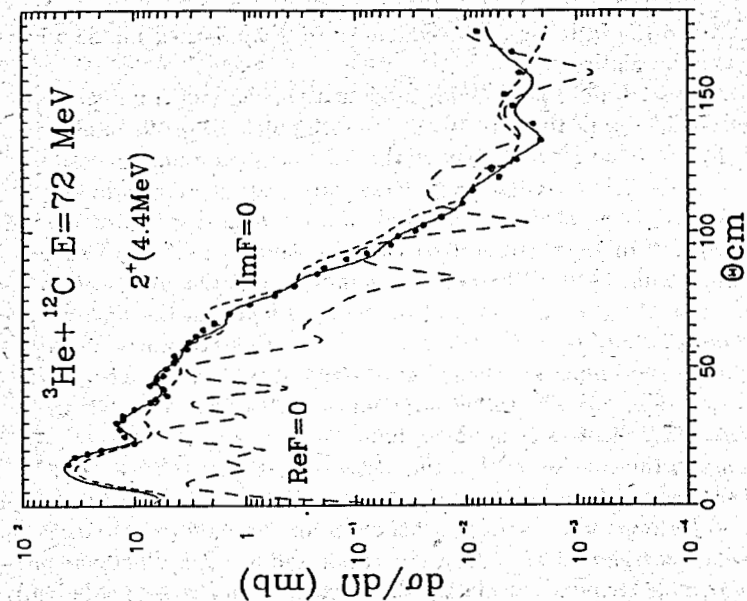


Fig 8b. The same as in Fig 2b for model independent form factor FB2.

factor contribution to the inelastic cross section (see a long dashed line in Fig. 8a), thus improving the description.

For the second procedure of form factor modification, the model independent real part practically coincides with the derivative of the A2 potential in the rainbow region thus providing the adequate reproduction of the rainbow maximum, while it is close to the derivative of the A4 potential around the strong absorption radius. (Special numerical investigations suggested that this could not be connected with a nonoptimal choice of the number N of Fourier-Bessel terms as in the case of [14]). This provides the necessary suppression both of the nearside component of the cross section and is equivalent to the role of the imaginary part of the form factor in the first procedure. The imaginary form factor, as is seen from Fig. 4, remains nonmonotonous but its contribution is much less important than that of the real part of the form factor (see a long dashed line in Fig. 8). The rather large inner parts of the form factors do not influence the scattering, due to strong absorption.

Thus, we come to the conclusion that the inelastic scattering ${}^3\text{He} + {}^{12}\text{C}(2^+)$, also in very fine details, can be reproduced by the A2 potential obtained in a simultaneous study of elastic scattering and the $({}^3\text{He}, t)$ reaction, if an appropriate form factor modification is done in the region of the strong absorption radius. This change requires us to go beyond the simple recipe of calculating the inelastic form factor as a derivative of the optical model potential. This result confirms the well-known sensitivity of inelastic scattering to the surface and tail of the form factor. The insensitivity of the $({}^3\text{He}, t)$ data [6] to the behaviour of the potential at large distances could be connected either with the special form of the charge-exchange form factor which is volume concentrated or with the fact that the $({}^3\text{He}, t)$ reaction cross section was not measured at very small angles.

Adding Fourier-Bessel series to the derivative form factor based on the A4 potential leaves it practically unchanged.

The necessity to abandon the derivative form factor recipe was also demonstrated by Bohlen et. al. [4] in the case of ${}^{12}\text{C} + {}^{12}\text{C}$ inelastic scattering. The difference for heavier ions from our work is that the form factor in that case had to be changed at smaller distances.

4 Conclusion

Inelastic scattering ${}^3\text{He} + {}^{12}\text{C}$ at $E=24$ MeV/A with excitation of low lying states of ${}^{12}\text{C}$ has been studied in a wide angular range. Our results seem to contain the following information.

1. The nuclear rainbow phenomenon is present also in this process. It has the same general features that characterize the nuclear rainbow in the elastic scattering. This result is also suggested by qualitative comparison with other existing data on inelastic scattering of light nuclei in the same energy range, but in contradiction with the ${}^{12}\text{C} + {}^{12}\text{C}$ measurements [4] where the nuclear rainbow was not substantiated in

the inelastic cross section.

2. A conventional DWBA inelastic scattering analysis based on an optical model potential found from fitting the elastic scattering data and an excitation form factor taken as a derivative of this potential, was performed. The potential A2 obtained from a simultaneous analysis of ${}^3\text{He}$ elastic scattering and $({}^3\text{He}, t)$ -reaction data [6] and which describes the rainbow features well, also reproduces the general features of the inelastic 2^+ and 3^- data. It cannot, however, reproduce the details of the angular distributions giving to rapid oscillatory structure. Coupled channels do not improve this significantly.

3. Some modification of the excitation form factor beyond the simple derivative recipe does, however lead to improvement. A model independent Fourier-Bessel analysis enable us to obtain a nearly perfect agreement with the inelastic data. The study of ${}^{12}\text{C} + {}^{12}\text{C}$ inelastic scattering [4] led us to a similar conclusion though it refers to a different spatial region.

4. We also tried to find out if a potential could be found which reproduces both the elastic and inelastic data, keeping the simple derivatives recipe for the excitation form factor. A candidate for such a potential A4 was found, but a significant improvement of the fit to the inelastic was obtained at the expense of a reduction in the quality of the elastic fit.

The study of inelastic scattering ${}^3\text{He} + {}^{12}\text{C}$ has added to our previous findings [2, 5, 6], and a consistent simultaneous analysis of elastic, inelastic scattering and reaction data has been obtained. This is vitally important for the determination of the nucleus-nucleus potential. The charge-exchange reactions data have demonstrated their sensitivity to the behaviour of the potential at short distances. Inelastic scattering seems to be sensitive to the slope of the potential in the strong absorption radial region and beyond.

Acknowledgments

One of the authors (J.S.V.) would like to thank for warm hospitality during many visits for JINR and Kurchatov institute during this project. The authors would also like to thank H.G. Bohlen and A. Ostrovskii for useful discussions.

References

- [1] Dem'yanova A.S., Ogloblin A.A., Sukharevsky V.V., *Tez. dokl. 35 sou. yad. spektrosk. and atomn. yadra, Leningrad, April(1985)360.*
- [2] Dem'yanova A.C., Ogloblin A.A., Ershov S.N., Gareev F.A., Korovin P.P., Goncharov S.A., Lyashko Yu.A., Adodin A.A., Bang J.M., *Nucl. Phys.*, A482 (1988)383
- [3] Dem'yanova A.S., Ogloblin A.A., Lyshko Yu.V., Adodin V.V., Burtebaev N., Ershov S.N., Gareev F.A., Korovin P.P., Bang J.M., Goncharov S.A., Vaagen J.S. *Phys. Rev.*, C38 (1988)1975
- [4] Bohlen H.G., Chen X.S., Cramer J.G., Frobrich P., Gebauer B., Lettau H., Miczaika A., von Oertzen W., Ulrich R., Wilpert T., *Z. Phys.*, A322 (1985)241
- [5] Ershov S.N., Gareev F.A., Kurmanov R.S., Svinareva E.F., Kazacha S.G., Dem'yanova A.C., Ogloblin A.A., Goncharov S.A., Vaagen J.S., Bang J.M., *Phys. Letts.*, Vol. B227 (1989)315
- [6] Dem'yanova A.C., Ogloblin A.A., Ershov S.N., Gareev F.A., Kurmanov R.S., Svinareva E.F., Goncharov S.A., Adodin V.V., Burtebaev N., Bang J.M., Vaagen J.S., *Phys. Scr.*, Vol. T32 (1990)89
- [7] Gluhov Yu.A., Dem'yanova A.S., Drosdov S.I., Zhukov M.V., Manko V.I., Novazki B.G., Ogloblin A.A., Sakuta S.B., Stepanov D.N., Chulkov L.V., *Sov. Yad. Physica*, vl.34, N 2(8), 1981, 312.
- [8] Tanabe T. etc., *J. of the Phys. Society of Japan*, vol.41, N2 (1976)1
- [9] Smith S.M. et. al., *Nucl. Phys.*, A207 (1973)273
- [10] Rebel H., Pesl R., Gils H.I., Friedman E., *Nucl. Phys.*, A368 (1981)61
- [11] Nadasen A., McMaster M., Fingal M. et. al., *Phys. Rev.*, C40(1989)1237
- [12] Goncharov S.A., Dem'yanova A.S., Ogloblin A.A., Lyashko Yu.V., Adodin V.V., Burtebaev N., Gareev F.A., Ershov S.N., *Tez. dokl. 38 sou. yad. spektrosk. and atom. yadra, Baku(1989)331.*
- [13] Brandan M.E., McVoy K.W., *Phys. Rev.*, C43 (1991)1140.
- [14] Kelly J. et. al., *Phys. Rev.*, C37 (1988)520.

Received by Publishing Department
on March 26, 1992.

Демьянова А.С. и др.

Рассеяние ^3He на ^{12}C и неупругий формфактор

E4-92-138

Представлены результаты измерения сечения неупругого рассеяния ^3He на ^{12}C при $E_{\text{He}} = 72$ МэВ с возбужденными низколежащими состояниями 2^+ , 3^- , 0^+ . Данные анализировались методом искаженных волн и методом связанных каналов, последний не приводит к существенным изменениям результатов, и мы пришли к выводу, что при неупругом рассеянии наблюдается ядерный радужный эффект. Основные черты неупругого углового распределения для состояний 2^+ и 3^- могут быть воспроизведены при использовании оптического модельного потенциала, ранее выбранного для реакции $(^3\text{He}, t)$ на мишенях $^{13},^{14}\text{C}$, только в том случае, если изменить формфактор, заданный в виде производной, в окрестности радиуса сильного поглощения. Теоретическое описание воспроизводит экспериментальные данные в деталях и может быть почти идеальным, если использовать более гибкий модельно-независимый формфактор. Обсуждается также альтернативный подход.

Работа выполнена в Лаборатории теоретической физики ОИЯИ.

Препринт Объединенного института ядерных исследований. Дубна 1992

Dem'yanova A.S. et al.

Scattering of ^3He on ^{12}C and Inelastic Form Factor

E4-92-138

Measurements of inelastic scattering of ^3He on ^{12}C at $E_{\text{He}} = 72$ MeV with excitation of low lying 2^+ , 3^- , 0^+ states of the target are reported. The data was analyzed both by DWBA and coupled channels approximation, the latter leading to only minor changes, and we argue that nuclear rainbow effects are present. It is possible to reproduce the main features of the 2^+ and 3^- inelastic angular distributions by means of the optical model potential previously selected for the reaction $(^3\text{He}, t)$ on $^{13},^{14}\text{C}$ targets, only if the derivative excitation form factors are modified in the vicinity of the strong absorption radius. The fit is improved in detail and can be made nearly perfect if more flexible model-independent form factors are employed. An alternative potential is also discussed.

The investigation has been performed at the Laboratory of Theoretical Physics, JINR.

Preprint of the Joint Institute for Nuclear Research, Dubna 1992